Modeling Adequacy for Studying Power Oscillation Damping in Grids with Wind Farms and Networked Control Systems (NCS)

Amirthagunaraj Yogarathinam, *Student Member, IEEE*, Jagdeep Kaur, *Student Member, IEEE*, and Nilanjan Ray Chaudhuri, *Member, IEEE*

***Abstract*—Network delays and data-dropouts could have a significant impact on Cyber-Physical System (CPS). In this paper power grid with large-scale deployment of distributed and networked Phasor Measurement Units (PMUs) and wind energy resources is considered as an example of CPS. Modeling and simulation studies are done in a power system with 151 dynamic states for stabilizing electromechanical oscillations using remote PMU signals under different rates of data dropout, fault locations, and different degrees of nonlinearity. To that end a centralized state-feedback controller is designed to modulate the current references of Doubly Fed Induction Generator (DFIG)-based wind farm (WF). Modeling adequacy studies of a representative subtransient model of the grid and the averaged model of DFIG-based WF along with the representation of packet drop in the communication network by a Gilbert-Elliot model and Bernoulli model is performed.**

***Index Terms*—Cyber-Physical System (CPS), Phasor Measurement Unit (PMU), Gilbert-Elliott Model, data-dropouts, communication, Networked Control System (NCS), Smart grid**

I. INTRODUCTION

TO meet the increase in load demand and to keep low-carbon footprint, renewable energy resources such as Wind Farms (WFs) and solar farms are integrated to the power system, which brings challenges to the operation of the power system. The utilities need ways to tackle these challenges in real time and respond to it. The Networked Control System (NCS) makes this possible with distributed networked sensors (i.e. Phasor Measurement Units (PMUs)).In a NCS the control and the feedback signals are exchanged amongst a multitude of sensors and actuators through a shared or dedicated band limited digital communication network in the form of data packets. However in a power system with large geographical span, leading to huge separation of the sensors and the actuators, the challenges of maintaining reliability within the NCS in the face of uncertainties like bandwidth limitations, data drop, and latency increases significantly.

Any communication network has the capability to handle a finite amount of information per unit time which creates a limitation in the operation of NCSs. Shannon's theory of the maximum bit rate that a communication channel can carry gives a motivation to find the minimum bit rate that is needed to stabilize a system performance through a feedback signal over a capacity communication channel. A lot of work [1], [2], [3] has been done to model the impact of data dropouts and delays in NCS but no comprehensive work has been reflected in the power systems literature. Most of research done on smart grid in the past, oversimplified the physical portion of the grid. In [4] the bandwidth (BW) restriction in the communication was dealt with in a deterministic framework and packet dropout was not considered. Singh *et-al* [5] represented packet data transmission process and probability of packet loss using an independent Bernoulli model in NCS for power system control. However, as mentioned in [5], the validity of Bernoulli model is questionable when the communication channel is congested. In addition, a clear gap has remained in understanding the implication of uncertainties in NCS cross-coupled with the nonlinearity of a large power grid with inverter-interfaced wind farms (WFs) on the reliable operation of the grid. Authenticity of the models of such systems is critical to achieve this understanding. Development of such a modeling framework and doing modeling adequacy studies is the subject matter of this work. In this paper, a detailed characterization of communication process with packet loss probability have been considered in NCS framework for power system control. A reduced order observer with linear quadratic regulator (LQR) based optimal control scheme is used to damp the inter area oscillations. Modeling adequacy study of the power system with inverter-interfaced WFs with different data dropout rates, fault locations and different degree of nonlinearity has been presented to find the interaction between the different layers of CPS.

The rest of the paper is organized as follows: The modeling of the Networked Controlled Power System (NCPS) is presented in section II. Section III discusses the design of centralized controller. A systematic approach for modeling adequacy study is laid out in section IV. Simulation results are presented in the section V, and section VI concludes the paper.

II. MODELING OF NCPS

NCPS consists of three major components, see Fig. 2, which are the Power system, the communication network and the controller, respectively.

A. Power System Model

In this work a 5-area 16-machine dynamic equivalent of the New England-New York system is considered. Synchronous

The authors are with Department of Electrical & Computer Engineering, North Dakota State University, Fargo, ND, USA (e-mail: *amirthagunaraj.yogar@ndsu.edu*, *jagdeep.kaur@ndsu.edu*, *nilanjanray.chaudhur@ndsu.edu*).

Financial support from NSF under grant award # 1464208 is gratefully acknowledged.

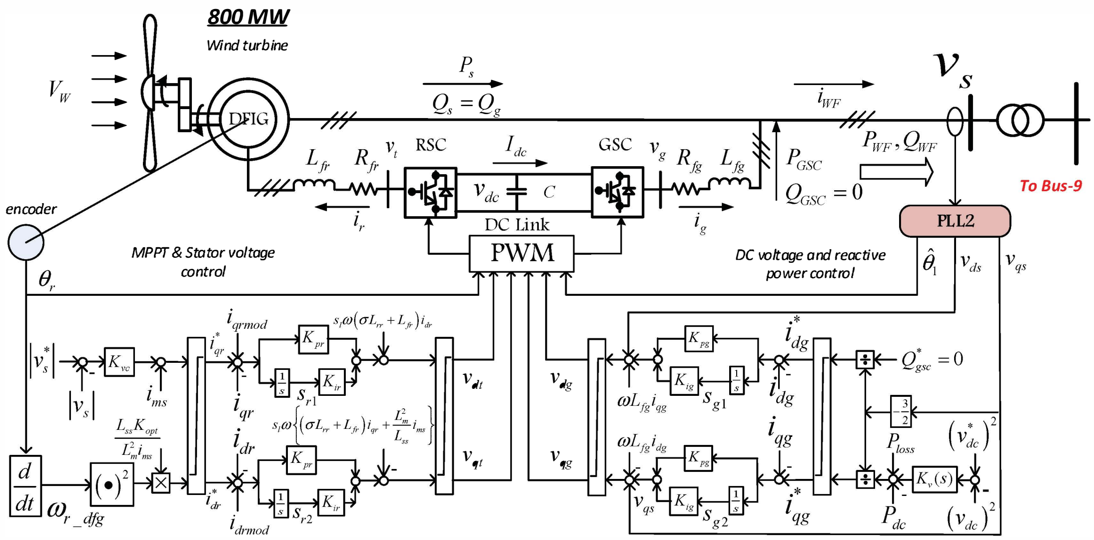

Fig. 1. Schematic of DFIG-based WF with its controllers. The WF is connected to the power system at the Bus-9

Generator (SG) G9 is replaced by a DFIG-based WF as shown in Fig. 3. The SGs are represented by a sixth-order subtransient model and eight of them (G1-G8) were equipped with IEEE DC1A excitation systems while the rest are with manual excitation. The active and reactive components of the loads have constant impedance characteristics. The AC network is modeled algebraically using Y-bus matrix as:

$$0 = [I] - [Y_{bus}][V_{bus}] \tag{1}$$

It takes the current injection vector $[I]$ of the power system components as input, and generates node voltage vector $[V]$ as output at each solution step.

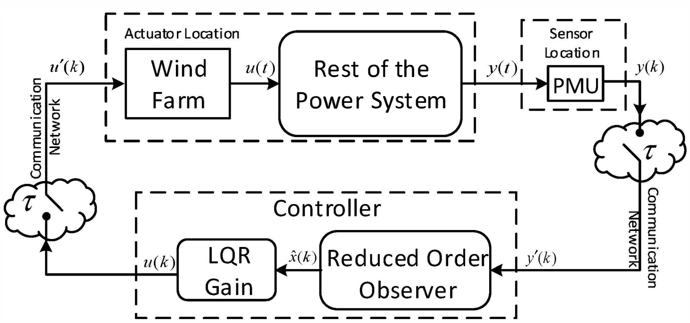

Fig. 2. Block diagram of the CPS architecture

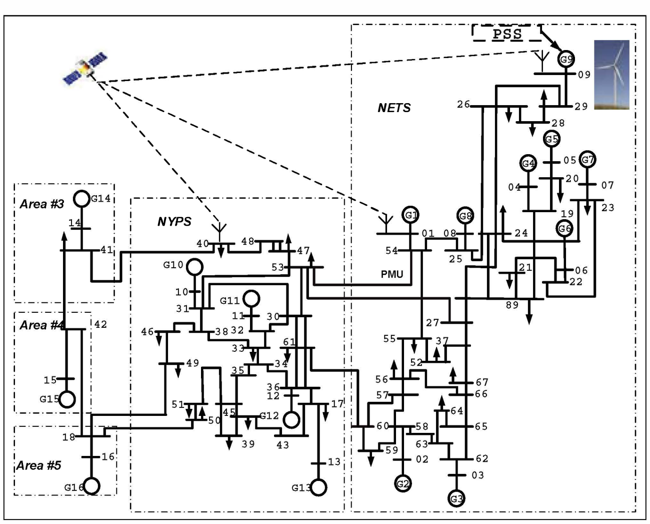

Fig. 3. 16-machine, 5-area equivalent representing New England New York power system. Wind Farm is located at bus 9.

The overall structure of aggregated DFIG-based WF is shown the Fig. 1, where the turbine-generator rotational dynamics is represented by a two-mass model. The wind speed is assumed to be constant and pitch angle control is neglected for the case study. The modeling of DFIG is done in a synchronously rotating d-q reference frame [6] with the d-axis leading the q-axis per IEEE convention. Stator transients of the induction machine are neglected and the tie-reactors of voltage source converters (VSCs), DC-link dynamics and the PLLs are included in the model. Standard vector control approach was considered for both rotor-side converter (RSC) and the grid-side convertor (GSC) controls [7]. For Maximum Power Point Tracking (MPPT) and the stator terminal voltage control for RSC, the stator flux is aligned with q-axis. As shown in the Fig. 1, for DC voltage control and reactive power control of GSC, the stator terminal voltage is aligned with the q-axis. The rotor current references can be modulated using i_{drmod} and i_{qrmod} (Fig. 1) to damp power oscillations.

The overal dynamic behavior of the power system can be expressed by a set of first order nonlinear differential and algebraic equations (DAEs) in the following form:

$$\dot{x} = \tau(x, z, u), 0 = g(x, z, u), y = h(x, z, u) \tag{2}$$

where τ and g are vectors of differential and algebraic equations and $x \in R^m$, $z \in R^q$, $u \in R^n$, and $y \in R^p$ are the vectors of state variables, algebraic variables, input and output, respectively.

B. Communication network and Data Dropout Models

To transmit a continuous-time signal over a communication network, the signal must be sampled and encoded in a digital format, transmitted over the network, and finally the data must be decoded at the receiver side. Dropout during the data transmission is always unpredictable. Reliable transmission protocols, such as Transmission Control Protocol (TCP), guarantees the eventual delivery of packets by sending the lost data again where as User Datagram Protocol (UDP) doesn't do so. However, TCPs are not appropriate for NCSs since the re-transmission of old data is generally not very useful [8], therefore in this analysis UDP is used. Uncertainties in the data traffic occurs in many forms such as bandwidth limitation, packet dropout, packet disorientation, latency and signal loss. This work focuses on the issues with dropout.

TABLE I
DIFFERENT DROPTOUT MODELS AND THEIR COMPLEXITY VS ACCURACY TRADEOFF

$Model$	$Parameter$	$Complexity$	$Simplification$
$Bernoulli$	p	$very\ low$	$k=1, h=0$
$Simple\ Gilbert$	p, r	low	$k=1, h \in \{0, 0.5\}$
$Gilbert$	p, r, h	$high$	$k=1$
$Gilbert-Elliott$	p, r, h, k	$very\ high$	$-$

Packet dropout over a network usually follows a stochastic process known as burst noise. Fig. 4 shows different stochastic models of packet dropout whose complexity and accuracy are shown in Table I [9]. The most complex and detailed 2-state Markov process called the Gilbert- Elliott model is shown in Fig. 4(a). This model considers two states: the good (G) and the bad (B) states. Each of them may generate errors as independent events with the state dependent error rates, $1-k$ and $1-h$ in the good and the bad states, respectively. The transition probabilities between the states are defined by, p: G-state to B-state, r: B-state to G-state. The stationary state probabilities P_G and P_B exist for $0 < (p, r) < 1$ from which the error rate P_E and the packet delivery rate (R) of the transmission channel can be obtained in steady state as:

$$\begin{aligned} &P_G = r/(p+r), P_B = p/(p+r) \\ &P_E = (1-k)P_G + (1-h)P_B \\ &R = (1-P_E) \times 100\% \end{aligned} \tag{3}$$

When $k=1$, the Gilbert- Elliott model is reduced to Gilbert model, Fig. 4(b). When $k=1$ and $h \in \{0, 0.5\}$ Gilbert model is reduced to simple Gilbert model, Fig. 4(c), and $k=1$, $h=0$ and $p+r=1$ gives the Bernoulli model, Fig. 4(d). This is the simplest dropout model.

The data packets are sent over the communication network to the centralized controller location and then to the actuator location. These signals are converted from digital to analog at the receiving end using digital to analog converters (DACs), in our system DACs are represented by zero-order-hold (ZOH) circuits. Consider the feedback signal from the PMU in the block diagram of Fig. 2, for which the signal $y(t)$ is sampled at times $\{t_k : k \in N\}$ and the samples $y(k) = y(t_k)$ are sent through the communication network. It is often assumed that when the packet containing the sample $y(k)$ is dropped the NCS utilizes the previous value of $y'(k)$. This corresponds to replacing the lossless network model by: $\forall k \in N$

$$y'(k) = \theta_k y(k) + (1-\theta_k) y'(k-1) \tag{4}$$

where $\theta_k = 0$ when there is a packet dropout at time k and $\theta_k = 1$ otherwise. Similarly the network model for control signal $u'(k)$ is modeled by:

$$u'(k) = \theta_{1k} u(k) + (1-\theta_{1k}) u'(k-1) \tag{5}$$

where θ_k and θ_{1k} are independent of each other. Here $u'(k)$ is the vector of modulating signals i_{drmod} and i_{qrmod} in Fig. 1.

Frequency of inter-area modes usually lie between $0.2-1.0$ Hz, therefore according to Nyquist-Shannon sampling theorem the minimum required sampling rate of the system is at least $2Hz$. In this work, the nominal rate of data sampling is assumed to be $10Hz$. The third element of the NCPS is the centralized controller which is described in the following section.

III. CENTRALIZED CONTROLLER DESIGN

DAEs in equation (2) describing the test system in Fig. 3 are linearized around a nominal point. The state space linearized model of the system is given by:

$$\begin{aligned} \Delta\dot{x}(t) &= A\Delta x(t) + B\Delta u(t) \\ \Delta y(t) &= C\Delta x(t) + D\Delta u(t) \end{aligned} \tag{6}$$

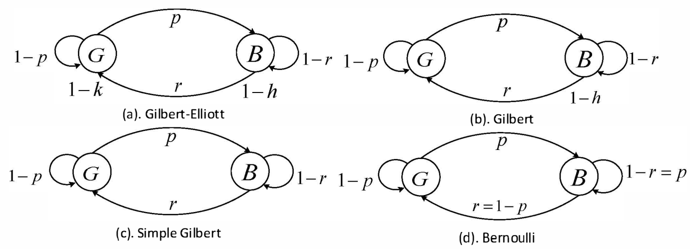

Fig. 4. Different data dropout models in the communication link.

where $A \in R^{m\times m}$, $B \in R^{m\times q}$ and $C \in R^{q\times m}$ are state matrix, input matrix and output matrix of the system, respectively. A reduced order model is derived without sacrificing the details of the inter area modes and poorly-damped modes of the system. The reduced order model is obtained by applying the balanced truncation method as shown in Fig. 5. The state space model of the reduced system can be written as:

$$\begin{aligned} \Delta\dot{x}(t) &= A_n\Delta x(t) + B_n\Delta u(t) \\ \Delta y(t) &= C_n\Delta x(t) + D_n\Delta u(t) \end{aligned} \tag{7}$$

where $A_n \in R^{n\times n}$, $B_n \in R^{n\times q}$ and $C_n \in R^{q\times n}$ and $n << m$

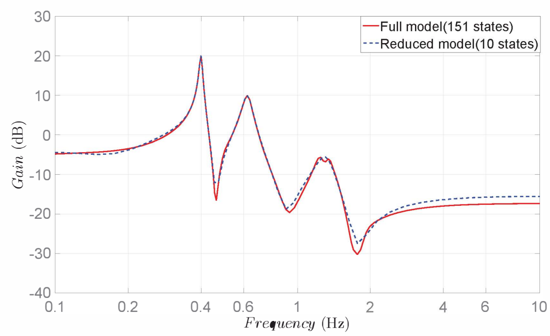

Fig. 5. Frequency response of the full model and the reduced model.

LQR-based Controller

The linearized system has four poorly damped inter-area modes and the objective of the controller is to damp these inter-area modes. To that end, a reduced order observer is used to estimate the state vector $\hat{x}(k)$ as shown Fig. 2. The state-space model of the observer is given by:

$$\begin{aligned} \hat{x}(k+1) &= A_n\hat{x}(k) + B_n u(k) + L(y'(k) - \hat{y}(k)) \\ \hat{y}(k) &= C_n\hat{x}(k) + D_n u(k) \end{aligned} \tag{8}$$

where, L is the observer gain. The state-feedback control law is given by:

$$u(k) = -K\hat{x}(k) \tag{9}$$

where, K, the state-feedback controller gain, is calculated using LQR to minimize the control effort. Selection of the feedback signal(s) play a major role in the effective damping controller design. In this case the real power flow through line 54-53 is selected as the feedback signal based on using residue magnitude-angle criteria as mentioned in [10].

IV. MODELING ADEQUACY STUDY

Modeling a framework of the power system with communication layer is a non-trivial task in absence of any established benchmark on modeling adequacy in the NCSs framework.

To study the modeling adequacy of the NCPS, different physical models with different communication layers are developed in MATLAB/Simulink platform.

A. Models of the physical layer of the system

For the modeling adequacy study, two types of positive sequence fundamental frequency phasor models have been developed,

☐ Type I model includes GSC and PLL dynamics of WF (Fig. 1).

☐ Type II model neglects these dynamics.

B. Models of Communication layer

The most accurate data drop model that is Gilbert-Elliott model and the most simplest model that is Bernoulli model are considered in studies along with the two types of physical layers mentioned before.

C. Nonlinearity and Uncertainties

The NCPS with different physical and cyber layers are analyzed under the following nonlinearity and uncertainties.

☐ Wider and narrow limits on RSC voltage v_{dt} and v_{qt} (Fig. 1).

☐ A self clearing fault at closer and remote locations from the WF.

☐ Different data receiving rates in the communication links.

Since Type I model with Gilbert-Elliott dropout model captures the most detailed description of the physical and the cyber layer of the NCPS, it is considered as a benchmark model for the analysis and named as Type I - Gilbert-Elliott, We follow the same notation for other three NCPS models as Type II - Gilbert-Elliott, Type I - Bernoulli and Type II - Bernoulli. Modeling adequacy of the cyber layer and the physical layer are studied by comparing system performance between Type I - Gilbert-Elliott and Type II - Gilbert-Elliott and between Type I - Gilbert-Elliott and Type I-Bernoulli, respectively, whereas modeling adequacy of physical layer coupled with cyber layer of the NCPS is studied by comparing the system performance between Type I - Gilbert-Elliott and Type II - Bernoulli models.

V. Simulation Results and Discussion

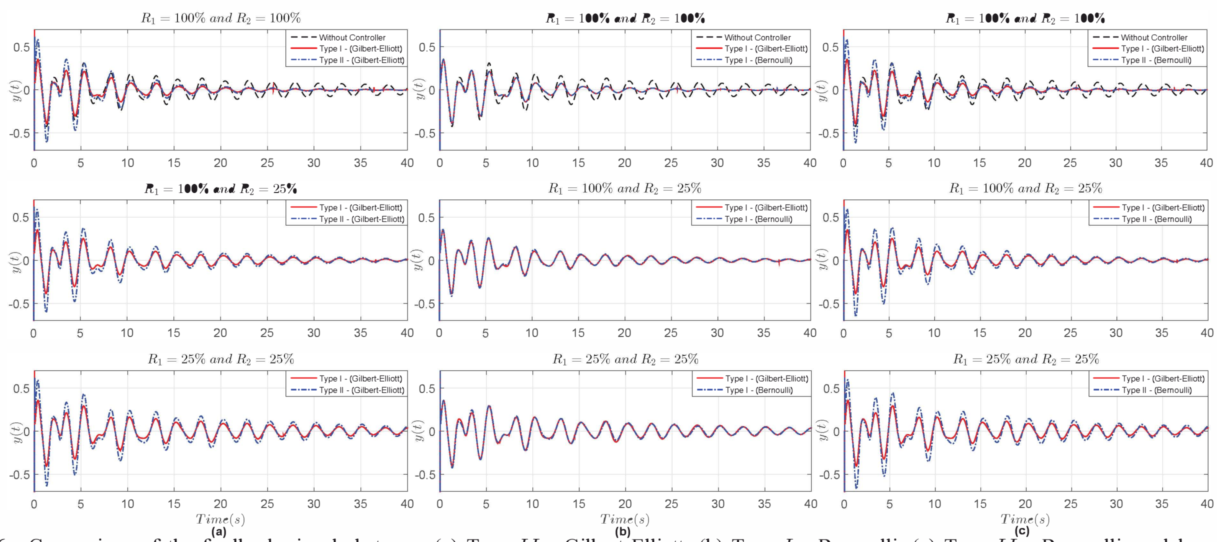

Fig. 6. Comparison of the feedback signals between (a) Type II - Gilbert-Elliott, (b) Type I - Bernoulli, (c) Type II - Bernoulli models with Type I - Gilbert-Elliott model when fault is at bus 28 and RSC voltage limit = $0.112p.u$ along with different data receiving rates in the communication channels.

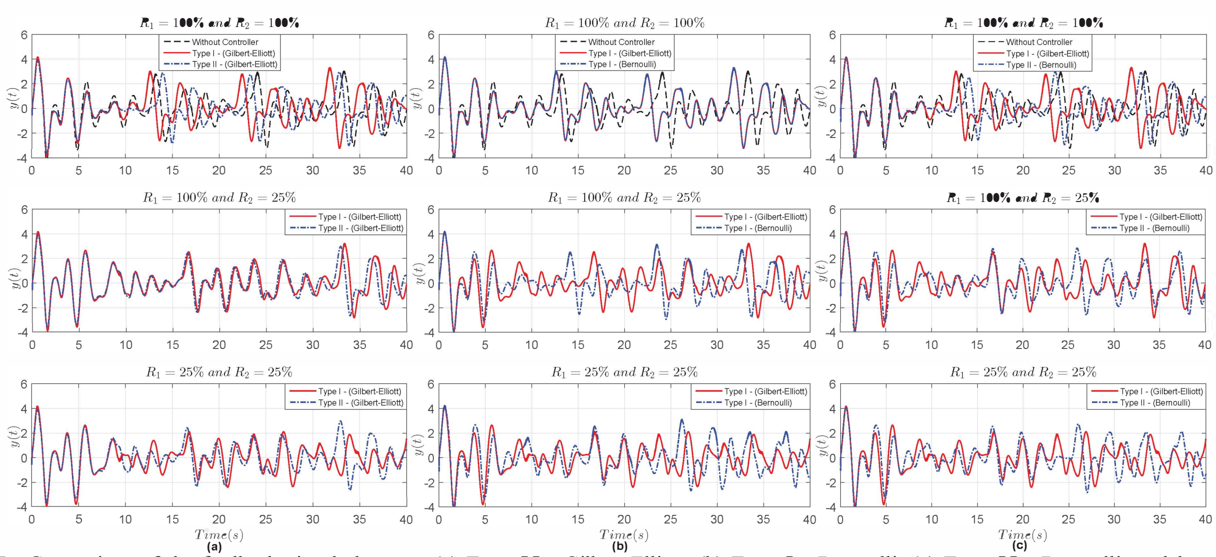

Fig. 7. Comparison of the feedback signals between (a) Type II - Gilbert-Elliott, (b) Type I - Bernoulli, (c) Type II - Bernoulli models with Type I - Gilbert-Elliott model when fault is at bus 60 and RSC voltage limit = $0.075p.u$ along with different data receiving rates in the communication channels.

TABLE II
MODELING ADEQUACY OF CYBER AND PHYSICAL LAYERS WITH DIFFERENT NONLINEARITY AND UNCERTAINTIES

Layer of NCPS	Nonlinearity					
	High			*Low*		
	Data Receiving Rates $(R_1 - R_2)$			*Data Receiving Rates* $(R_1 - R_2)$		
	$100\% - 100\%$	$100\% - 25\%$	$25\% - 25\%$	$100\% - 100\%$	$100\% - 25\%$	$25\% - 25\%$
Physical Layer Type-II-Gilbert-Elliott	*Inadequate*	*Marginally Adequate*	*Inadequate*	*Adequate*	*Adequate*	*Adequate*
Cyber Layer Type-I-Bernoulli	*Adequate*	*Inadequate*	*Inadequate*	*Adequate*	*Adequate*	*Adequate*
Cyber and Physical Layer Type-II-Bernoulli	*Indequate*	*Inadequate*	*Inadequate*	*Adequate*	*Adequate*	*Adequate*

The simulation results with a self-clearing three-phase fault for 20 ms at bus 28 with wider RSC voltage limit and bus 60 with narrow RSC voltage limit along with different data receiving rates are shown in Fig. 6 and Fig. 7, respectively. R_1 and R_2 are the data receiving rates of the control input signals $u'(k)$ and the feedback signal $y'(k)$, respectively (see Fig. 2). The NCPS is also studied with the same fault at bus 28 with narrow RSC voltage limit and bus 60 with wider RSC voltage limit but, due to the space constrains, these are not shown here. The simulation is carried out in MATLAB/Simulink using the solver ode23t (mod. Stiff/Trapezoidal) with variable time step and relative tolerance of 10^{-6}.

Table II summarizes the adequacy of the models of different NCPS layers for different nonlinearity and uncertainties. It can be observed from Fig. 6 that all the models i.e. Type II - Gilbert-Elliott which represents physical layer, Type I - Bernoulli and Type II - Bernoulli are adequate to capture the dynamics of the cyber and physical layer of the NCPS for low degree of nonlinearity. The Type II - Gilbert-Elliott model is inadequate in capturing the system dynamics with high degree of nonlinearity and its adequacy is dependent on the uncertainties in the cyber layer, Fig. 7(a). Type I - Bernoulli which represent the cyber layer is inadequate when degree of nonlinearity and uncertainties is increased but it is adequate in the absence of uncertainties in receiving the data as expected, see Fig. 7(b) while the Type II - Bernoulli model shows inadequacy under high nonlinearity condition, see Fig. 6(c). This reveals that the adequacy of NCPS framework with large power system and communication layer is dependent on the degree of nonlinearity of the physical layer, coupled with the uncertainties in the cyber layer.

VI. CONCLUSION

A modeling framework of cyber-physical system has been developed where equivalent of New England-New York area power system with one synchronous generator replaced by DFIG-based inverter-interfaced WF with its controls and dynamics represents the physical layer while, the cyber layer is modeled by using one of the two models for data droupout in communication link which is Gilbert-Elliott model and Bernoulli model. The LQR based centralized controller is used to damp the inter-area oscillations following a fault. The modeling adequacy study of this system with different data dropout rates, fault locations and different degree of nonlinearity reveals that the adequacy is dependent on the degree of nonlinearity of the physical layer, coupled with the uncertainty in the cyber layer. Our ongoing research is focused on more extensive study of modeling adequacy evaluation of such systems.

VII. APPENDIX: LIST OF NOTATIONS

R: Turbine radius
ρ: Air density
$K_{opt} = 0.5\rho\pi R^5 C_{Popt}/\lambda_{opt}^3$
C_{Popt}: Optimum power coefficient
λ_{opt}: Optimum tip-speed-ratio
R_r/R_s, L_r/L_s: Rotor/Stator resistance/leakage inductance
L_m: Mutual inductance
i_{qg}/i_{dg}: q/d-axis GSC current
i_{qr}/i_{dr}: q/d-axis RSC current
v_{qs}/v_{ds}: q/d-axis DFIG bus voltage
$v_{qt}/v_{qg}, v_{dt}/v_{dg}$: q/d-axis RSC/GSC voltage
i_{ms}: Magnetizing current
$R_{fr}/R_{fg}/L_{fr}/L_{fg}$: RSC/GSC filter resistance/inductance
$s_{r1}/s_{g1}, s_{r2}/s_{g2}$: RSC current controller states
K_{vc}: Droop constant in RSC voltage controller
$K_{ir}/K_{ig}, K_{pr}/K_{pg}$: RSC/GSC controller parameters
$K_v(s)$: DC voltage controller
$L_{ss} = L_s + L_m$
$L_{rr} = L_r + L_m$
$\sigma = 1 - L_m^2/(L_{ss}L_{rr})$
Rest of the notations are self-explanatory from Fig. 1.

REFERENCES

[1] L. A. Montestruque and P. Antsaklis, "Stability of model-based networked control systems with time-varying transmission times," *IEEE Transactions on Automatic Control*, vol. 49, no. 9, pp. 1562–1572, 2004.

[2] L. A. Montestruque and P. J. Antsaklis, "On the model-based control of networked systems," *Automatica*, vol. 39, no. 10, pp. 1837–1843, 2003.

[3] M. S. Branicky, "Stability of switched and hybrid systems," in *Proceedings of the 33rd IEEE Conference on Decision and Control, 1994*, vol. 4, 1994, pp. 3498–3503 vol.4.

[4] N. R. Chaudhuri, D. Chakraborty, and B. Chaudhuri, "An architecture for facts controllers to deal with bandwidth-constrained communication," *IEEE Transactions on Power Delivery*, vol. 26, no. 1, pp. 188–196, 2011.

[5] A. Singh, R. Singh, and B. Pal, "Stability Analysis of Networked Control in Smart Grids," *IEEE Transactions on Smart Grid*, vol. 6, pp. 381–390, 2015.

[6] P. Kundur, *Power system stability and control*, ser. The EPRI power system engineering series. New York; London: McGraw-Hill, 1994.

[7] R. Pena, J. C. Clare, and G. M. Asher, "Doubly fed induction generator using back-to-back PWM converters and its application to variable-speed wind-energy generation," *IEE Proceedings on Electric Power Applications*, vol. 143, no. 3, pp. 231–241, 1996.

[8] J. Hespanha, P. Naghshtabrizi, and Y. Xu, "A survey of recent results in networked control systems," *Proceedings of the IEEE*, vol. 95, pp. 138–162, 2007.

[9] G. Hasslinger and O. Hohlfeld, "The gilbert-elliott model for packet loss in real time services on the internet," 2008, pp. 1–15.

[10] S. Ray, B. Chaudhuri, and R. Majumder, "Appropriate signal selection for damping multi-modal oscillations using low order controllers," 2008, pp. 1–7.